A large conjugative *Acinetobacter baumannii* plasmid carrying the *sul2* sulphonamide and *strAB* streptomycin resistance genes

Mohammad Hamidian[*1], Stephanie J. Ambrose[1], and Ruth M. Hall[1]

[1]School of Life and Environmental Sciences, The University of Sydney, NSW 2006, Australia

Running title: Conjugative *Acinetobacter baumannii* plasmids carrying *sul2*

Keywords: *Acinetobacter* conjugative plasmid, Tn*6172*, MITE-297, *sul2, strA, strB.*

*Corresponding author: Mohammad Hamidian

Mailing address:

School of Life and Environmental Sciences,

Molecular Bioscience Building G08,

The University of Sydney, NSW 2006, Australia.

Phone: +61-2-9351-6030

Fax: +61-2-9351-5858

E-mail: mohammad.hamidian@sydney.edu.au

Abstract

Acinetobacter baumannii is an important nosocomial pathogen that often complicates treatment because of its high level of resistance to antibiotics. Though plasmids can potentially introduce various genes into bacterial strains, compared to other Gram-negative bacteria, information about the unique *A. baumannii* plasmid repertoire is limited. Here, whole genome sequence data was used to determine the plasmid content of strain A297 (RUH875), the reference strain for the globally disseminated multiply resistant *A. baumannii* clone, global clone 1(GC1). A297 contains three plasmids. Two known plasmids were present; one, pA297-1 (pRAY*), carries the *aadB* gentamicin, kanamycin and tobramycin resistance gene and another is an 8.7 kb cryptic plasmid often found in GC1 isolates. The third plasmid, pA297-3, is 200 kb and carries the *sul2* sulphonamide resistance gene and *strAB* streptomycin resistance gene within Tn*6172* and a *mer* mercuric ion resistance module elsewhere. pA297-3 transfered sulphonamide, streptomycin and mercuric ion resistance at high frequency to a susceptible *A. baumannii* recipient, and contains several genes potentially involved in conjugative transfer. However, a relaxase gene was not found. It also includes several genes encoding proteins involved in DNA metabolism such as partitioning. However, a gene encoding a replication initiation protein could not be found. pA297-3 includes two copies of a Miniature Inverted-Repeat Transposable Element (MITE), named MITE-297, bracketing a 77.5 kb fragment, which contains several IS and the *mer* module.

Several plasmids related to but smaller than pA297-3 were found in the GenBank nucleotide database. They were found in different *A. baumannii* clones and are wide spread. They all contain either Tn*6172* or a variant in the same position in the backbone as Tn*6172* in pA297-3. Some related plasmids have lost the segment between the MITE-297 copies and retain only one MITE-297. Others have segments of various lengths between two MITE-297 copies, and these can be derived from the region in pA297-3 via a deletion adjacent to IS

related to IS*26* such as IS*1007* or IS*1007-like.* pA297-3 and its relatives represent a third type of conjugative *Acinetobacter* plasmid that contributes to the dissemination of antibiotic resistance in this species.

55 # 1. Introduction

56 *Acinetobacter baumannii* is a member of the ESKAPE group, six pathogens that are
57 the main causes of hospital-acquired antibiotic-resistant infections globally (Rice, 2008). In *A.*
58 *baumannii*, resistance genes are often located in the chromosome in genomic resistance
59 islands (Blackwell et al., 2016; Chan et al., 2015; Holt et al., 2016; Nigro and Hall, 2016;
60 Wright et al., 2016). However, recent reports indicate the significance of *A. baumannii*
61 plasmids as vehicles to introduce antibiotic resistance genes such as *oxa23* and bla_{NDM}
62 leading to resistance to the front line carbapenem antibiotics (Hamidian et al., 2014a;
63 Hamidian et al., 2014b; Jones et al., 2014; Nigro and Hall, 2016; Nigro et al., 2015). *A.*
64 *baumannii* strains carry plasmids of several different types (Bertini et al., 2010) that differ
65 from the plasmids found in most Gram-negative pathogens. These include small cryptic
66 plasmids, small plasmids that carry resistance genes and medium to large size plasmids
67 carrying one or more antibiotic resistance genes. Despite the importance of *A. baumannii*
68 plasmids and the large number of complete plasmid sequences available in GenBank (Bertini
69 et al., 2010), not a lot of information about the *A. baumannii* plasmid repertoire, the functions
70 they carry and their transferability is available. Several *rep*Aci6 plasmids carrying the *aphA6*
71 amikacin resistance gene or the *oxa23* carbapenem resistance gene or both have been shown
72 to be conjugative (Hamidian and Hall, 2014; Hamidian et al., 2014a; Hamidian et al., 2014b;
73 Nigro et al., 2015). Another type of conjugative plasmid is associated with bla_{NDM}, which
74 confers resistance to all ß-lactams except aztreonam (Jones et al., 2015; Zhang et al., 2013).

75 The multiply antibiotic-resistant *A. baumannii* isolate A297 (RUH875), which belongs
76 to ST231/ST109 (Oxford scheme) and ST1 (Institut Pasteur) (Holt et al., 2016) and is the type
77 strain for global clone 1 (GC1). It was isolated in 1984 in Dordrecht, the Netherlands, from a
78 urinary tract infection (Dijkshoorn et al., 1996) and later renamed A297 (Hamouda et al.,
79 2010). It is resistant to ampicillin/sulbactam, piperacillin, sulfamethoxazole, trimethoprim,

gentamicin, tobramycin, kanamycin, neomycin, streptomycin, spectinomycin and tetracycline (Nigro et al., 2011). A297 carries AbaR21, a resistance island in the *comM* gene in the chromosome, which contains *tetA*(A), *catA1,* bla_{TEM}, *aphA1b, dfrA5* and *sul1* conferring resistance to tetracycline, chloramphenicol, ampicillin, kanamycin, trimethoprim and sulphonamides, respectively (Nigro et al., 2011). The 6 kb plasmid pRAY*, carrying the *aadB* gene, accounts for the tobramycin, kanamycin and gentamicin resistance (Hamidian et al., 2012; Holt et al., 2016). However, the *strAB* and *sul2* genes, which are rarely seen in GC1 isolates, were also found in A297 in the configuration ISAba1-*sul2*-CR2-*strB*-*strA* but the context and location of this structure was not determined (Nigro et al., 2011).

We recently reported a 132,632 bp plasmid in a ST25 strain carrying the ISAba1-*sul2*-CR2-*strA*-*strB* structure in a class III transposon, designated Tn*6172* (Hamidian and Hall, 2016). This plasmid carries a set of genes encoding potential transfer functions. However, it was not conjugative (Hamidian and Hall, 2016). Here, whole genome sequence data of A297 reported recently (Holt et al., 2016), bioinformatics analyses and conventional PCR-sequencing approaches were used to examine the location of the ISAba1-*sul2*-CR2-*strA*-*strB* structure.

2. Materials and Methods

2.1. Genome sequencing, PCR amplification and plasmid assembly

The draft genome sequence of A297 (determined using Illumina HiSeq) has been reported previously (Holt et al., 2016). The draft genome, contains 92 contigs and is available in the GenBank WGS database under the accession number FBWR01000000.

pA297-3 was assembled from 28 contigs that were identified using a number of approaches. Briefly, the contig containing the *sul2* and *strAB* genes was recovered using Standalone BLAST. A set of criteria including looking for sequences found in pD4

105 (Hamidian and Hall, 2016), and the sequence of insertion sequences found at the end of
106 contigs were used. Target site duplications generated by IS and the direction of IS were used
107 to order contigs. Contigs identified were then joined using PCR, with a combination of
108 published primers and primers designed here (Table S1), and the products were sequenced.
109 The final sequence was assembled in Sequencher 5.2.3 (Gene Codes Corporation, Ann Arbor,
110 MI, USA). Copy numbers were estimated by dividing the coverage of plasmid contigs by that
111 of chromosomal contigs.
112
113 *2.2. Annotations*
114 The plasmid sequence was annotated automatically using Prokka (Seemann, 2014)
115 with the default cut off of 80 amino acid (aa) followed by manual annotation of other DNA
116 features such as the insertion sequences and transposons. The plasmid sequence was also
117 inspected using ORF Finder (www.ncbi.nlm.nih.gov/projects/gorf/) to confirm the genes/orfs
118 (open reading frames) found by the annotation program. BLASTp and Pfam searches were
119 used to examine individual orfs, with no function assigned by Prokka. The entire plasmid
120 sequence was also inspected using tBLASTn. GC skew analysis using DNA Plotter was used
121 to find a possible replication initiation site (origin of replication).
122 Final GenBank submission file was prepared using the tbl2asn software, available at
123 http://www.ncbi.nlm.nih.gov/genbank/tbl2asn2/. Figures were drawn to scale using Gene
124 Construction Kit (GCK 4.0.3), SnapGene® Viewer 2.8.1 and Adobe Illustrator CS6.
125
126 *2.3. Conjugation*
127 A derivative of the rifampicin resistant strain *A. baumannii* ATCC 17978^{rif} (Hamidian
128 et al., 2014a), which had lost pAB3 spontaneously and was therefore sulphonamide sensitive
129 was isolated as follows and designated 17978^{rif}-A. Briefly, ATCC 17978^{rif} was grown without

selection and cells were plated on L-agar. Resulting colonies were patched onto Muller-Hinton Agar and MHA with sulfamethoxazole. Colonies that grew only on MHA without sulfamethoxazole were screened by PCR for *sul2* and a pAB3 sequence to ensure that the plasmid had been lost.

Conjugation experiments were carried out using 17978^{rif}-A as recipient. Briefly, equal amounts of overnight cultures of the donor (A297) and recipient (17978^{rif}-A) were mixed and incubated on an L-agar plate overnight. Cells were re-suspended and diluted in 0.9% saline, and transconjugants were selected by plating on MHA plates containing rifampicin (100 mg/L) and sulfamethoxazole (100 mg/L). Transfer frequency (transconjugants/donor) was the average of 3 determinations. To confirm that only sulfamethoxazole and streptomycin resistance were transferred, potential transconjugants were purified and checked for growth on L-agar containing kanamycin (20 mg/L) and tetracycline (10 mg/L), to which the donor was resistant and the recipient susceptible. Transconjugants identified in this way were screened further for antibiotic resistance phenotypes, as well as with specific PCRs that could distinguish the donor from recipient. Resistance to mercuric chloride was tested by patching fresh colonies onto L-agar supplemented 20 mg/L $HgCl_2$.

2.4. Bioinformatics

Sequences belonging to several plasmids related to pA297-3 found in the GenBank non-redundant and the Whole Genome Shotgun (WGS) databases were retrieved and studied here. Amongst several plasmids found in WGS, only the ones that appeared to be assembled in a single contig were included in this study. Multi-locus sequence types (MLST; Institut Pasteur scheme (http://pubmlst.org/abaumannii/)) of the associated isolates were determined *in silico* using their genome sequence data retrieved from GenBank (http://www.ncbi.nlm.nih.gov/genome).

155

156 *2.5. Nucleotide sequence accession numbers*

157 The complete sequence of the plasmids pA297-1 (pRAY*), pA297-2 and pA297-3
158 were annotated and deposited in GenBank under accession numbers KU869529, KU869528,
159 and KU744946, respectively.

160

161 ## 3. Results

162 *3.1. pA297-3, a plasmid carrying the* sul2 *and* strAB *genes in Tn*6172

163 In the A297 draft genome, the ISAba1-*sul2*-CR2-*strB*-*strA* structure was found within
164 Tn*6172*, a transposon that we recently defined in pD4 (GenBank accession number
165 KT779035), which is a plasmid from an Australian ST25 isolate (Hamidian and Hall, 2016).
166 Tn*6172* was in a 119 kb contig (contig 10; see Table S2) and the sequences surrounding
167 Tn*6172* were identical to the flanking sequence of Tn*6172* in pD4. The rest of contig 10 was
168 almost identical to the backbone of pD4 but it did not include any of the four ISAba25-like
169 insertions found in pD4. This indicated the presence of a similar plasmid in A297 that was
170 designated pA297-3. One end of contig 10 contained ~60 bp of IS*1008* and the other end
171 included a novel sequence (see below) found in pD4. The remaining 3.5 kb of pD4 was found
172 in four contigs (115, 48, 97 and 5; Table S2) and it was possible to link the IS*1008* end of
173 contig 10 to the novel sequence in a 3.5 kb PCR product that included the four contigs.
174 However, attempts to link ends of contig 10, which generated a 4.8 kb product from pD4,
175 failed. This suggested that there might be an additional segment in pA297-3.

176

177 *3.2. A novel miniature inverted-repeat transposable element (MITE) in pD4*

178 The novel sequence found at one end of contig 10 was found to be part of a 502 bp
179 segment of pD4 (bases 101947-102448 in KT779035) that has properties similar to some

transposons (Fig. 1). This element is bounded by 26 bp terminal inverted repeats (IR) that start with TGT and further copies of the internal part of this IR were found near the ends. These features are similar to those of Tn*6019*/Tn*6022* family transposons, which form the backbone of AbaR type and AbaR4 islands respectively (Hamidian and Hall, 2011). However, the sequences of this element or its IRs were not related to any known transposon or IS. It appears that this element is a remnant of an old transposon, which has lost its middle segment as it only encodes a 102 aa protein of unknown function. These characteristics place this structure in the category of miniature inverted-repeat transposable elements (MITE). Therefore, hereafter, it will be referred to as MITE-297.

3.3. An additional segment in pA297-3 between two MITEs

Using the MITE sequence as a query, four additional contigs (contig 97, 5, 81 and 4; Table S2) were identified. Contig 5 contained the internal sequence of the MITE-297 and the others ended with ~60 bp from one of the MITE-297 ends. These contigs were ordered, as shown in Fig. 1, by PCR and sequencing. Each MITE-297 is flanked by a 5 bp target site duplication (TGAAG or CTTCT) indicative of transposition into these two positions (Fig. 1). Hence, there are two MITE-297 copies in pA297-3 separated by an additional segment that is not present in pD4. The single MITE in pD4 is flanked by TGAAG and CTTCT (Fig. 1). Hence, pD4 is derived from a larger plasmid that contained two MITE-297 copies and the segment between them was lost via homologous recombination between two the MITE copies (Fig. 1).

A second IS*1008* was found at the other end of contig 4 (see Fig. 1), and it was linked to a 354 bp contig (contig 30; Table S2) that included the opposite end of IS*1008*. Assembling the additional segment of pA297-3 was complicated due to the complex nature of this segment. However, a similar strategy, using the fragments of repeated elements at the end of

contigs to suggest possible joins, was used repeatedly to assemble the rest of the additional segment. An additional 20 contigs ranging in size from 150 bp to 19.6 kb were incorporated.

Several IS were found between the two MITE-297 copies, some of which had internal deletions or were IS remnants (Table 1, Fig. 2). IS*1007,* IS*1007-like* and IS*1008* are each relatives of IS*26* (72%-74% identical). Three novel insertion sequences, ISAba34, ISAba35 and ISAba37, were identified in this segment (Table 1, Fig. 2). These three IS belong to different IS families but were found to generate a target site duplication of 3 bp each. The properties of the IS found in the backbone of pA297-3 are listed in Table 1. The segment between the two MITE-297 copies contains several genes/orfs encoding various proteins including oxidoreductases, dehydrogenases, transcriptional regulators and proteins involved in DNA metabolism such as RecN (involved in recombination and repair) or Tsx (nucleoside-specific channel forming protein) (Fig. 2, Table S4). Only orfs with a predicted function are shown in Figure 2 and a complete annotation of this segment is in supplementary Table S4.

3.4. pA297-3, a 200 kb conjugative plasmid

The final assembly of pA297-3 required 28 of the 92 contigs in the draft genome assembly (Table S2). pA297-3 could be distinguished from pD4 by the presence of a 77994 bp segment consisting of a 77.5 kb novel sequence and an additional MITE-297 copy. The size of pA297-3 was found to be 200633 bp and a map is shown in Fig. 2. The copy number of pA297-3 was equivalent to that of the chromosome. pA297-3 was shown to transfer sulphonamide and streptomycin resistance into the rifampicin-resistant recipient strain 17978^{rif}-A (Table 3). The transfer frequency was high at 7.20×10^{-2} transconjugants/donor (average of 3 determinations). PCR amplification of DNA from a single transconjugant was used to confirm that all segments of the assembled sequence were present. The potentially

mobilizable plasmid pRAY* was not co-transferred as the transconjugants tested were susceptible to aminoglycosides (tobramycin, gentamicin and kanamycin) (Table 3).

3.5. The mer *module*

The additional segment contains a *mer* operon that includes *merD, A*, *C, P, T* and the regulatory gene *merR* (Fig. 3). Functionality of this *mer* operon could not be tested while pA297-3 is in A297 as there is another *mer* operon in the AbaR21 located in the chromosome (Nigro, 2011 #2;Holt et al., 2016). However, the streptomycin and sulfamethoxazole resistant 17978^{rif}-A transconjugants carrying pA297-3 grew on L-agar containing 20 mg/L $HgCl_2$, indicating that the *mer* operon in pA297-3 (Fig. 2) can confer resistance to mercuric ions. 17978^{rif}-A cells, without pA297-3, did not grow on L-agar plates supplemented with $HgCl_2$.

The entire *mer* operon was found to be almost identical (differs by 2 bp) to a hybrid *mer* module found in an unnamed 141 kb plasmid (GenBank accession number CP014652) from the environmental *Acinetobacter* sp. strain DUT-2 recovered from marine sediments. Apart from a 36 bp deletion that was found in DUT-2, 78 bp before the 3'-end of *merD*, the regions surrounding the *mer* operon, extending for 25 kb on the left and 8.3 kb on the right, were also 99.9% identical to regions flanking the *mer* operon in pA297-3. In addition, several fragments of pDUT-2 ranging in size from 1.6 to 10 kb, were also found to be related (94-99% identity) to segments of the region between the two MITE-297 copies in pA297-3. However, the rest of the backbone was not related to pA297-3. Additional environmental plasmids, e.g. pKLH204 (GenBank accession number AJ487050) and pKLH203 (GenBank accession number AJ486855) (Kholodii et al., 2004), were also found to contain hybrid *mer* regions almost identical (3-5 bp difference) to that in pA297-3. However, in pA297-3 there is a 349 bp deletion in the 3'-end of *merD* compared to those plasmids. Analysis revealed that the deletion is likely to have arisen via a recombination event involving a very short, 8 bp

(CCGCAGCA) repeat present within *merD*. The *mer* operon has a hybrid structure with sequence derived from pMER610 (GenBank accession number Y08993) at either end of the module (99.9% DNA identity; bases 118468-119411 and bases 121394-122093 of KU744946) (Fig. 3). The middle segment is derived from Tn*1696* (GenBank accession number Y09025) with 99.9% DNA identity. However, the segments intervening Tn*1696* and pMER610 derived sequences are novel.

3.6. The segment shared by pA297-3 and pD4

Annotation of the part of the pA297-3 backbone (i.e. Tn*6172* not included) shared with pD4 is presented in the supplementary Table S3. This segment contains *parA* and *parB* genes, encoding plasmid partitioning proteins. It also contains a series of other genes involved in DNA metabolism (shown by gray arrows in Fig. 2). However, despite extensive searches (see Methods), we were unable to find a gene encoding a potential replication initiation protein. Functions needed for stable inheritance must be present in this segment but finding them will require further work. Examination of the GC bias suggested that the replication origin maybe in the vicinity of the primase and *traW* genes (marked by an arrow in Fig 2).

This segment includes *umuDC* genes encoding a Y-family translesion synthesis DNA polymerase (TLP). TLP are responsible for most of the mutagenesis resulting from exposure to DNA damaging agents such as UV light (Norton et al., 2013).

This segment also contains a set of 13 genes encoding conjugative transfer proteins, shown yellow in Fig.2. The gene products all showed 23-30% aa identity to proteins encoded by the IncI plasmid R64 (*tra* operon) (GenBank accession number AP005147) that are part of the MPF_I conjugation system (Smillie et al., 2010). Table 2 lists amino acid (aa) identities of the product of the pA297-3 transfer genes compared to those of R64. However, the full complement of transfer genes known to be essential for transfer of R64 (Smillie et al., 2010)

was not found in pA297-3. In particular, a potential relaxase (Mob) was not found and whether further genes are required remains to be established.

3.7. Plasmids related to pA297-3 in other Acinetobacter *genomes*

Several plasmids in the size range of 122-216 kb, with backbones closely related to those of pA297-3 and pD4 were found in the GenBank databases (Table 4). The strains belonged to various sequence types (ST) and were from different countries indicating that these plasmids have a wide geographical distribution. In all cases Tn*6172* or a variant form of Tn*6172* was found in precisely the same spot in the plasmid backbone as in pA297-3 (bases 64245-75963; KU744946) and pD4 (Fig. 4). The resistance regions in the Tn*6172* variants found in pAB04-1, pIOMTU433, and in plasmids found in B11911 and SP1917 (here designated pB11911 and pSP1917) are larger, ranging in size from 39 to 57 kb, and include several additional resistance genes (Table 4).

Each plasmid included large segments with 99.9% DNA identity to the main part of the backbone of pA297-3. However, different IS insertions, a few insertions/deletions and fragments with lower identities (92-98%) distinguish each of the backbones (Fig.4). Amongst the plasmids listed in Table 4, pIOMTU433, pSP1917 and pB11911 also had a segment of different lengths between two MITE-297 copies. In pSP1917 and pB11911 (Fig. 4B), a 19 kb portion segment, including the *mer* operon, has been removed, by an IS*1007* mediated deletion. Compared to others, pB11911 and pSP1917 contain 1 and 2 copies of IS*10A*, respectively. In pIOMTU433, the IS*1007-like* has deleted 39.8 kb on its left hand side such that IS*1007-like* is now separated from the MITE-297 copy, on the left, by only 49 bp (Fig. 4B).

3.8. A297 contains two small plasmids, pA297-1 (pRAY) and pA297-2*

304 We have previously reported that A297 contains a copy of the tobramycin, gentamicin
305 and kanamycin resistance plasmid pRAY* (Hamidian et al., 2012). Here, we found that the
306 6078 bp sequence of pA297-1 (pRAY*) (copy number 3-4) differs from pRAY* (GenBank
307 accession number JQ904627), found in the strain D36 (Hamidian and Hall, 2011), at 1
308 position.
309 A297 also harbours a 8731 bp cryptic plasmid, named pA297-2 (copy number 7-8),
310 that is of the type frequently found in GC1 isolates, such as pA85-2 (GenBank accession
311 number KJ477078) (Hamidian et al., 2014b) and pAb-G7-1 (GenBank accession number
312 KJ586856) in G7 (Hamidian et al., 2014a). pA297-2 differs from pAb-G7-1 and pA85-2 at 1
313 and 2 positions, respectively.
314

315 ## 4. Discussion

316 The GC1 reference strain A297 (RUH875) isolated in 1984 contains 3 plasmids, two
317 of which had been characterized previously. pA297-1(pRAY*) is a 6078 bp plasmid carrying
318 the *aadB* gene (Hamidian et al., 2012), and pA297-2 a 8731 bp cryptic plasmid, which is
319 identical to ones found in most GC1s (Hamidian et al., 2014a; Hamidian et al., 2014b).
320 pA297-3 is a 200 kb conjugative plasmid that can transfer sulphonamide, streptomycin and
321 mercury resistance to a recipient at high frequency.
322 pA297-3 includes the *sul2* and *strAB* genes in Tn*6172*, which is also found in the
323 same position in pD4 (Hamidian and Hall, 2016) and in several relatives found in GenBank.
324 Other related plasmids have Tn*6172* or a variant of Tn*6172* in the same position. Many of the
325 smaller plasmids arose from pA297-3 (Fig. 4) via homologous recombination between the
326 two MITE-297 copies. A *mer* module found in the region between the two MITE-297 in
327 pA297-3 has been removed via a deletion caused by IS*1007*, in pB11911 and pSP1917, and
328 IS*1007-like* in pIOMTU433 (Fig. 4). Hence, the pA297-3 configuration is clearly ancestral.

It appears that the segment between the MITE-297 copies that is lost is not essential for replication. However, no gene encoding a protein related to a known replication initiation protein was found in the remainder. This is unusual for a large plasmid and experimental work will be needed to identify the region essential for plasmid replication, which should include the replication initiation genes. pA297-3 encodes further proteins potentially involved in DNA metabolism including ParA and ParB plasmid partitioning proteins, Pri, a putative second strand synthesis primase, RecN, involved in recombination and repair, Tsx, a nucleoside-specific channel forming protein, and TopA, which is a DNA topoisomerase. pA297-3 also encodes UmuD and UmuC, which are closely related to UmuD and UmuC (81% and 91% aa identity, respectively) proteins in ATCC 17978 that have been shown to be induced after DNA damage (Norton et al., 2013).

A modest number of genes likely to be involved in conjugative transfer were detected in the span that is shared with pD4 (Table 2) and pA297-3 encodes a putative TrbC, which is related to conjugation coupling factors. However, a *mob* gene encoding a relaxase was not found. pD4 was not able to transfer but this maybe due to the presence of an ISAba25-like inserted in the primase gene (located between *traY* and *traW*). A related but smaller plasmid, pAB3 (GenBank accession number CP012005), that does not include the region between MITE-297 copies, has been shown to be conjugative (Weber et al., 2015). Hence, the functions encoded by the segment between MITE-297 copies may have little impact on the conjugative ability of these plasmids. However, as the backbone of pAB3 differs significantly from that of pD4 and pA297-3, this needs to be confirmed by testing further smaller plasmids that lack the segment between MITE-297 copies.

MITE structures are present in genomes of diverse bacteria and often < 200 bp in length (Delihas, 2008). A MITE of >400 bp has been reported in *Acinetobacter* (Domingues et al., 2011; Gallagher et al., 2015; Gillings et al., 2009). However, MITE-297 was not related

to this or any other MITE described to date. It appears that it belongs to the same family as the *tni* transposons (class III) such as Tn*6019* and Tn*6022* found in *Acinetobacter* species (Hamidian and Hall, 2011) as it is bounded by 26 bp IRs, starts with TGT and ends with ACA, includes additional copies of the internal end of the IR at each end and generates a 5 bp target site duplication.

Plasmids belonging to this family were found in isolates belonging to different clonal types indicating that they have spread widely (Table 4). The fact that A297 is an early GC1 isolate indicates these plasmids have been present in the *A. baumannii* population since the early days of multiple resistance. However, later GC1 isolates do not include the *sul2* gene or a pA297-3 (Holt et al., 2016) family plasmids. Plasmids in this family have been shown to carry two genes encoding TetR-type regulators (see Fig. 2) that suppress the type VI secretion system, reducing the ability to compete with other bacteria (Weber et al., 2015). It appears that, over time, a number of insertion/deletion and recombination events have diverged these plasmids.

Funding

This study and M. H. were supported by NHMRC Project Grant 1079616.

References

Bertini, A., Poirel, L., Mugnier, P. D., Villa, L., Nordmann, P., Carattoli, A., 2010. Characterization and PCR-based replicon typing of resistance plasmids in *Acinetobacter baumannii*. Antimicrob. Agents. Chemother. 54**,** 4168-77.

Blackwell, G. A., Hamidian, M., Hall, R. M., 2016. The IncM plasmid R1215 is the source of chromosomally-located regions containing multiple antibiotic resistance genes in the globally disseminated *Acinetobacter baumannii* GC1 and GC2 clones. mSphere. 8, 1. 10.1128/mSphere.00117-16.

Chan, A. P., Sutton, G., DePew, J., Krishnakumar, R., Choi, Y., Huang, X. Z., Beck, E., Harkins, D. M., Kim, M., Lesho, E. P., Nikolich, M. P., Fouts, D. E., 2015. A novel method of consensus pan-chromosome assembly and large-scale comparative analysis reveal the highly flexible pan-genome of *Acinetobacter baumannii*. Genome. Biol. 21, 16, 143. 10.1186/s13059-015-0701-6.

Delihas, N., 2008. Small mobile sequences in bacteria display diverse structure/function motifs. Mol. Microbiol. 67**,** 475-81.

Dijkshoorn, L., Aucken, H., Gerner-Smidt, P., Janssen, P., Kaufmann, M. E., Garaizar, J., Ursing, J., Pitt, T. L., 1996. Comparison of outbreak and nonoutbreak *Acinetobacter baumannii* strains by genotypic and phenotypic methods. J. Clin. Microbiol. 34**,** 1519-1525.

Domingues, S., Nielsen, K. M., da Silva, G. J., 2011. The $bla_{\text{IMP-5}}$ carrying integron in a clinical *Acinetobacter baumannii* strain is flanked by miniature inverted-repeat transposable elements (MITEs). J. Antimicrob. Chemother. 66**,** 2667-8.

Gallagher, L. A., Ramage, E., Weiss, E. J., Radey, M., Hayden, H. S., Held, K. G., Huse, H. K., Zurawski, D. V., Brittnacher, M. J., Manoil, C., 2015. Resources for Genetic and Genomic Analysis of Emerging Pathogen *Acinetobacter baumannii*. J. Bacteriol. 197**,** 2027-35.

Gillings, M. R., Labbate, M., Sajjad, A., Giguere, N. J., Holley, M. P., Stokes, H. W., 2009. Mobilization of a Tn*402*-like class 1 integron with a novel cassette array via flanking miniature inverted-repeat transposable element-like structures. Appl. Environ. Microbiol. 75**,** 6002-4.

Hamidian, M., Hall, R. M., 2011. AbaR4 replaces AbaR3 in a carbapenem-resistant *Acinetobacter baumannii* isolate belonging to global clone 1 from an Australian hospital. J. Antimicrob. Chemother. 66**,** 2484-91.

Hamidian, M., Hall, R. M., 2014. pACICU2 is a conjugative plasmid of *Acinetobacter* carrying the aminoglycoside resistance transposon Tn*aphA6*. J. Antimicrob. Chemother. 69**,** 1146-8.

Hamidian, M., Hall, R. M., 2016. The resistance gene complement of D4, a multiply antibiotic-resistant ST25 *Acinetobacter baumannii* isolate, resides in two genomic islands and a plasmid. J. Antimicrob. Chemother. 71**,** 1730-2.

Hamidian, M., Holt, K. E., Pickard, D., Dougan, G., Hall, R. M., 2014a. A GC1 *Acinetobacter baumannii* isolate carrying AbaR3 and the aminoglycoside resistance transposon Tn*aphA6* in a conjugative plasmid. J. Antimicrob. Chemother. 69**,** 955-8.

Hamidian, M., Kenyon, J. J., Holt, K. E., Pickard, D., Hall, R. M., 2014b. A conjugative plasmid carrying the carbapenem resistance gene $bla_{\text{OXA-23}}$ in AbaR4 in an extensively resistant GC1 *Acinetobacter baumannii* isolate. J. Antimicrob. Chemother. 69**,** 2625-8.

Hamidian, M., Nigro, S. J., Hall, R. M., 2012. Variants of the gentamicin and tobramycin resistance plasmid pRAY are widely distributed in *Acinetobacter*. J. Antimicrob. Chemother. 67**,** 2833-6.

Hamouda, A., Evans, B. A., Towner, K. J., Amyes, S. G., 2010. Characterization of epidemiologically unrelated *Acinetobacter baumannii* isolates from four continents by use of multilocus sequence typing, pulsed-field gel electrophoresis, and sequence-based typing of $bla_{\text{OXA-51-like}}$ genes. J. Clin. Microbiol. 48**,** 2476-83.

Holt, K., Kenyon, J. J., Hamidian, M., Schultz, M. B., Pickard, D. J., Dougan, G., Hall, R., 2016. Five decades of genome evolution in the globally distributed, extensively antibiotic-resistant *Acinetobacter baumannii* global clone 1. Microbial Genomics. 2**,** 10.1099/mgen.0.000052.

Jones, L. S., Carvalho, M. J., Toleman, M. A., White, P. L., Connor, T. R., Mushtaq, A., Weeks, J. L., Kumarasamy, K. K., Raven, K. E., Torok, M. E., Peacock, S. J., Howe, R. A., Walsh, T. R., 2015. Characterization of plasmids in extensively drug-resistant *Acinetobacter* strains isolated in India and Pakistan. Antimicrob. Agents Chemother. 59**,** 923-9.

Jones, L. S., Toleman, M. A., Weeks, J. L., Howe, R. A., Walsh, T. R., Kumarasamy, K. K., 2014. Plasmid carriage of $bla_{\text{NDM-1}}$ in clinical *Acinetobacter baumannii* isolates from India. Antimicrob. Agents Chemother. 58**,** 4211-3.

Kholodii, G., Mindlin, S., Gorlenko, Z., Petrova, M., Hobman, J., Nikiforov, V., 2004. Translocation of transposition-deficient (TndPKLH2-like) transposons in the natural environment: mechanistic insights from the study of adjacent DNA sequences. Microbiology. 150**,** 979-92.

Nigro, S. J., Hall, R. M., 2016. Loss and gain of aminoglycoside resistance in global clone 2 *Acinetobacter baumannii* in Australia via modification of genomic resistance islands and acquisition of plasmids. J. Antimicrob. Chemother. 10.1093/jac/dkw176.

Nigro, S. J., Holt, K. E., Pickard, D., Hall, R. M., 2015. Carbapenem and amikacin resistance on a large conjugative *Acinetobacter baumannii* plasmid. J. Antimicrob. Chemother. 70**,** 1259-61.

Nigro, S. J., Post, V., Hall, R. M., 2011. The multiresistant *Acinetobacter baumannii* European clone I type strain RUH875 (A297) carries a genomic antibiotic resistance island AbaR21, plasmid pRAY and a cluster containing ISAba1-*sul2*-CR2-*strB*-*strA*. J. Antimicrob. Chemother. 66**,** 1928-30.

Norton, M. D., Spilkia, A. J., Godoy, V. G., 2013. Antibiotic resistance acquired through a DNA damage-inducible response in *Acinetobacter baumannii*. J. Bacteriol. 195**,** 1335-45.

Rice, L. B., 2008. Federal funding for the study of antimicrobial resistance in nosocomial pathogens: no ESKAPE. J. Infect. Dis. 197**,** 1079-81.

Seemann, T., 2014. Prokka: rapid prokaryotic genome annotation. Bioinformatics. 30**,** 2068-9.

Smillie, C., Garcillan-Barcia, M. P., Francia, M. V., Rocha, E. P., de la Cruz, F., 2010. Mobility of plasmids. Microbiol. Mol. Biol. Rev. 74**,** 434-52.

Weber, B. S., Ly, P. M., Irwin, J. N., Pukatzki, S., Feldman, M. F., 2015. A multidrug resistance plasmid contains the molecular switch for type VI secretion in *Acinetobacter baumannii*. Proc. Natl. Acad. Sci. U S A. 112**,** 9442-7.

Wright, M. S., Iovleva, A., Jacobs, M. R., Bonomo, R. A., Adams, M. D., 2016. Genome dynamics of multidrug-resistant *Acinetobacter baumannii* during infection and treatment. Genome Med. 8**,** 26. 10.1186/s13073-016-0279-y.

Zhang, W. J., Lu, Z., Schwarz, S., Zhang, R. M., Wang, X. M., Si, W., Yu, S., Chen, L., Liu, S., 2013. Complete sequence of the $bla_{\text{NDM-1}}$ carrying plasmid pNDM-AB from *Acinetobacter baumannii* of food animal origin. J. Antimicrob. Chemother. 68**,** 1681-2.

Table 1

Insertion sequences found in the backbone of pA297-3.

IS[a]	Length	Copies present	IS family	DR[b]	IR[c]	Sequence range[d]
IS*1008*	820	2	IS*6*	-	17	88899-89718 166827-167648
IS*1007*	819	1	IS*6*	-	18	122129-122947
IS*1007-like*	818	1	IS*6*	-	16	132337-133118
ISAha2	1040	3	IS*5*	-	16	join (91412-91953, 92461-92958)[e] 106628-107487[f] 111775-112814
ISAba37	1031	1	IS*5*	3	18	98096-98965
ISAba34	1309	1	IS*3*	3	26	94363-95671
ISAba35	1282	1	IS*150*	3	27	99754-101035
ISAcsp1	3736	3[g]	Tn*3*	-	46	152788-156523 165771-166144[h] 166477-166826[i]

[a] insertion sequence.
[b] direct repeats generated in pA297-3.
[c] inverted repeats.
[d] based on GenBank accession number KU744946.
[e] interrupted by a MITE-copy.
[f] this ISAha2 copy is 860 bp as it includes 180 bp deletion.
[g] one complete and two partial copies.
[h] 347 bp of the left end of ISAcsp1.
[i] 350 bp of the right end of ISAcsp1.

Table 2

Essential transfer genes in R64 compared to their corresponding genes in pA297-3

Gene	Product size R64 [a] (aa)	Product size pA297-3 [b] (aa)	Protein identity (%)	Function [c]
traB	177	-	-	Transcription termination factor
traC	227	-	-	Putative positive regulator
traI	272	272	25 (39/156)[d]	Lipoprotein
traJ	382	429	23 (79/339)	Nucleotide binding protein
traK	96	-	-	Transfer protein
sogL	1255	618	28 (34/123)	SogL DNA primase
traL	115	-	-	Signal peptide
traM	230	238	23 (54/233)	Thick pilus formation/DNA transfer
traN	327	376	30 (83/277)	Signal peptide
traO	429	543	26 (40/154)	Thick pilus formation/DNA transfer
traP	234	-	-	Thick pilus formation/DNA transfer
traQ	175	-	-	Thick pilus formation/DNA transfer
traR	134	-	-	Thick pilus formation/DNA transfer
traT	266	-	-	Thick pilus formation/DNA transfer
traU	1014	1090	23 (248/1060)	Nucleotide binding protein
traV	204	-	-	Thick pilus formation/DNA transfer
traW	400	377	23 (26/114)	Lipoprotein
traX	194	-	-	Thick pilus formation/DNA transfer
traY	745	759	25 (81/325)	Integral membrane protein
trbA	402	456	20 (41/206)	Thick pilus formation/DNA transfer
trbB	356	-	-	Essential for efficient transfer
trbC	763	912	27 (151/551)	Nucleotide binding protein
nikA	98	-	-	NikA *oriT*-specific DNA binding protein;
nikB	899	-	-	NikB relaxase

[a] GenBank accession number: AP005147.

[b] GenBank accession number: KU744946.

[c] functions predicted are based on PMID:10760136.

[d] numbers in brackets indicate amino acid (aa) identities.

Table 3. Antibiotic resistance profiles of donor, recipient and transconjugants

Isolate	Annular radius of inhibition zone (mm) [a]								
	Sm	Su	Tc	Tp	Km	Nm	Gm	Tm	Rif
A297 [b]	2	0	1	0	0	4	3	3	8
17978^{rif}-A [c]	6	7	7	5	7.5	7	7	7	0
Transconjugant 1	3.5	0	8	6	7	7	8	8	0
Transconjugant 2	3	0	7	6	7	6.5	8	8	0
Transconjugant 3	2.5	0	7	6	7.5	6.5	8	8	0

[a] Sm, streptomycin; Su, sulphonamide; Tc, tetracycline; Tp, trimethoprim; Km, kanamycin; Nm, neomycin; Gm, gentamicin; Tm, tobramycin; Rif: rifampicin,

[b] donor

[c] recipient.

Table 4

Properties of strains carrying plasmids related to pA297-3.

Strain	Plasmid	ST (IP)	Plasmid size (bp)	Country	Date	Tn	Resistance genes in Tn	Additional backbone insertions [a]	Accession number
A297 (RUH875)	pA297-3	1	200633	Netherlands	1984	*6172*	*sul2, strA, strB*	IS*1008* (2x), ISAha2, ISAha2Δ (2x), ISAba34, ISAba35, ISAba37, IS*1007,* IS*1007-like,* ISAcsp1, ISAcsp1Δ (2x), MITE-297 (2x)	KU744946
D4	pD4	25	132632	Australia	2006	*6172*	*sul2, strA, strB*	ISAba25-like (4x), IS*1008*, ISAha2Δ, MITE	KT779035
OIFC143	pIOFC143-128	25	127663	USA	2003	*6172*	*sul2, strA, strB*	ISAba25-like (2x), IS*1008*, ISAha2Δ, MITE	AFDL01000008
Naval-18	pNaval18-131	25	130660	USA	2006	*6172*:: ISEc57	*sul2, strA, strB*	ISAba25-like (2x), ISAba125, IS*1008*, ISAha2Δ, MITE	AFDA02000009
OIFC137	pIOFC137-122	3	122461[b]	USA	2003	*6172*	*sul2, strA, strB*	IS*1008*, ISAha2Δ, MITE	AFDK01000004
OIFC109	pIOFC109-122	3	122469[b]	USA	2003	*6172*	*sul2, strA, strB*	IS*1008*, ISAha2Δ, MITE	ALAL01000013
Naval-13	pNaval-13	3	122566	USA	2006	*6172*	*sul2, strA, strB*	IS*1008*, ISAha2Δ, MITE	AMDR01000015
OIFC065	pOIFC065	136	122569	USA	2003	*6172*	*sul2, strA, strB*	IS*1008*, ISAha2Δ, MITE	AMFV01000043
IS-116	pIS-116	136	122568	Iraq	2008	*6172*	*sul2, strA, strB*	IS*1008*, ISAha2Δ, MITE	AMGF01000021
Ab04-mff	pAB04-1	10	169023	Canada	2012	new 1[c]	*sul2* (2x), *tetA*(B), *mph2*, *mel, armA*, *sul1*(2x), *cmlA5*, bla_{PER}, *arr-2, strA, strB*	IS*1008*, ISAha2Δ, MITE	CP012007
IOMTU433	pIOMTU433	622	188296	Nepal	2013	new 2 [d]	*sul2*, *mph2*, *mel, armA*, *sul1*(2x), *cmlA5*, bla_{PER}, *arr-2, strA, strB*	IS*1008* (2x), ISAha2Δ, MITE (2x), IS*1007*-like, ISAcsp1	AP014650
SP1917	pSP1917 [e]	149	214979 [f]	India	2014	new 3	*sul2* , *mph2*, *mel, armA*, *sul1*(2x), *sul2*, *cmlA5*, *arr-2, strA, strB*	ISAcsp1, ISAcsp1Δ(2x), IS*10A* (2x) ISAba34, ISAba35, ISAba37, IS*1008* (2x), IS*1007,* IS*1007-like,* MITE (2x), ISAha2Δ	LFYW01000002
B11911	pB11911	149	216870 [f]	India	2014	new 4	*sul2* , *mph2*, *mel, armA*, *sul1*(2x), *sul2*, *cmlA5*, bla_{PER}, *arr-2, strA, strB*	ISAcsp1, ISAcsp1Δ(2x), IS*10A* ISAba34, ISAba35, ISAba37, IS*1008* (2x), IS*1007,* IS*1007-like,* MITE (2x), ISAha2Δ	LFYX01000002

[a] This column includes insertions found in the backbone other than Tn*6172* and its variants. MITE in all plasmids listed in the table is identical to MITE-297.

[b] pIOFC109-122 and pIOFC137-122 include a 170 bp deletion in their backbone compared to pIOFC143-128, pNaval18-131, pD4 and pA297-3.

[c] the resistance region includes a Tn*6172* backbone with an additional 39383 bp segment containing CR1(2x), CR2 (2x), IS*26*(3x), ISEc28, ISEc29, IS*10a,* and *sul2*, *tetA*(B), *mph2*, *mel, armA*, *sul1*(2x), *sul2*, *cmlA5*, bla_{PER} and *arr-2* resistance genes

[d] The Tn is similar to that in pAB04-1. However, compared to that in pAB04-1, the entire *tni* module of Tn*6172,* one copy of *sul2*, CR2, ISAba1 and *tetA*(B) are removed via IS*26*-mediated deletion. The remaining part also lacks the IS*26* adjacent to the *intI1*Δ- *arr-2* segment. Besides, a segment containing a copy of CR2 and its adjacent 3481 bp containing 3 hypothetical proteins are also missing in pIOMTU433 compared to the corresponding region in pAB04-1.

[e] plasmid name assigned here.

[f] Estimated size.

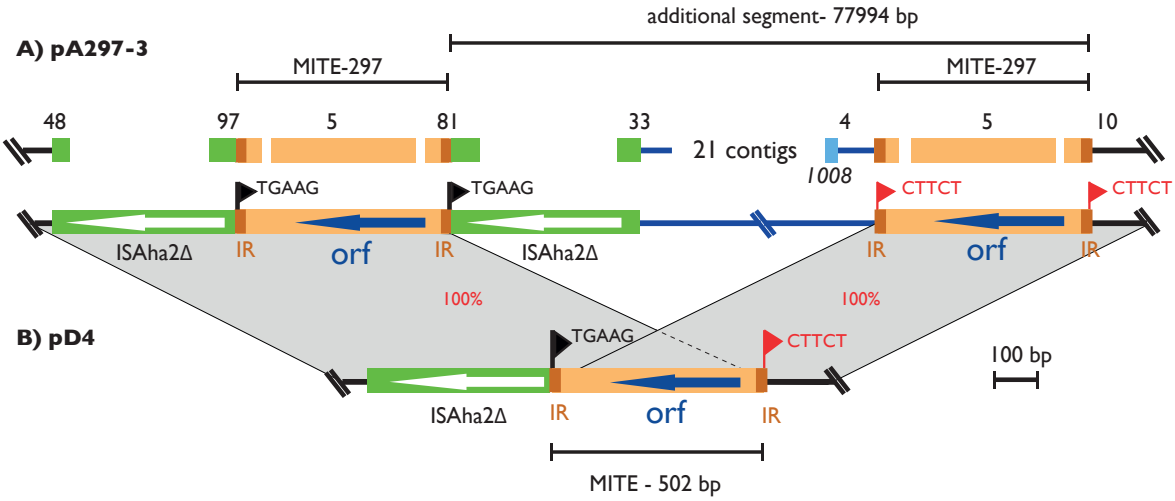

Fig. 1. The structure of the region surrounding the MITE-297 (Miniature Inverted Repeat Transposable Element) copies in the backbone of pA297-3 and pD4. A) shows MITE-297 copies in pA297-3 and their flanking regions. Contigs linked to assemble regions around the MITE-297 copies are also shown above. B) indicates the structure of the region surrounding the MITE-297 in pD4. The horizontal lines colored black represent plasmid backbone. The horizontal dark blue line indicates the additional 77.9 kb segment in pA297-3. Arrows indicate the orientation of genes. The boxes colored orange indicate the MITE-297 structure surrounded by thick brown vertical lines representing Inverted repeats (IR). Triangles colored black and red indicate direct repeats (DR) and the shade of grey indicate the regions with identical sequences. The scale bar is also shown.

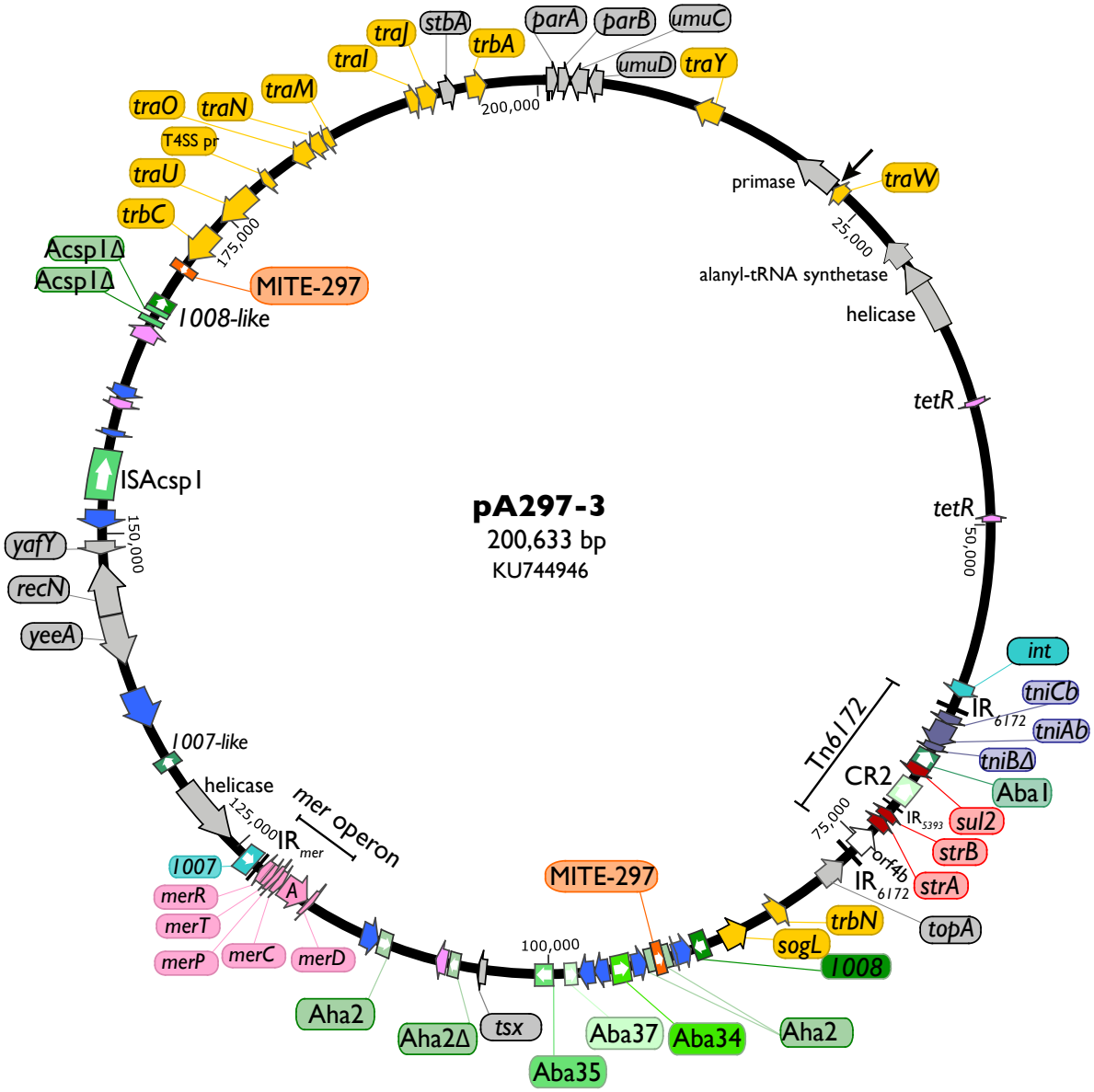

Fig. 2. Circular map of pA297-3 drawn to scale from GenBank accession number KU744946. Arrows represent the orientation and extent of genes and open reading frames. Open reading frames with no predicted function are not shown. For complete annotation see Tables S3 and S4. Straight lines inside the map of pA297-3 indicate the extent of the *mer* and Tn*6172*. Inverted repeats of Tn*6172,* and the *mer* are indicated by vertical bars and insertion sequences (IS) are shown with filled boxes colored different shades of green and white arrows inside the boxes indicate the direction of the *tnp* genes. Arrows colored yellow represent the *tra* genes, which are involved in plasmid transfer. Gray arrows represent genes/orfs involved in DNA metabolism. Arrows colored blue indicate open reading frames involved in various pathways.

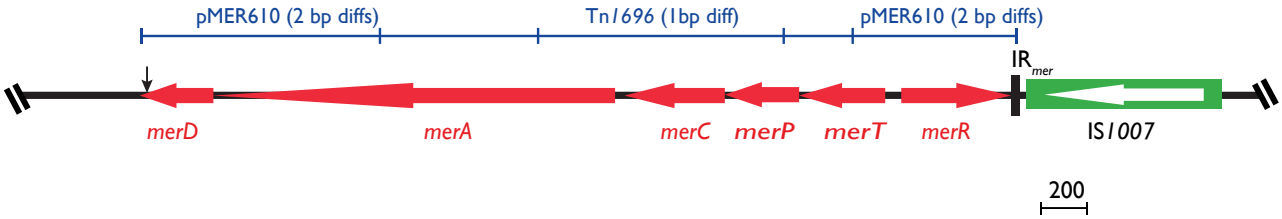

527 **Fig. 3.** Schematic of the *mer* operon found in pA297-3. Thick solid line indicates the
528 backbone of pA297-3 and red arrows show the extent and direction of the *mer* genes. The
529 green box represents IS*1007* and the white arrow inside is the tnp_{1007} gene. The sequence
530 source of each section is indicated above. The scale bar is also shown.

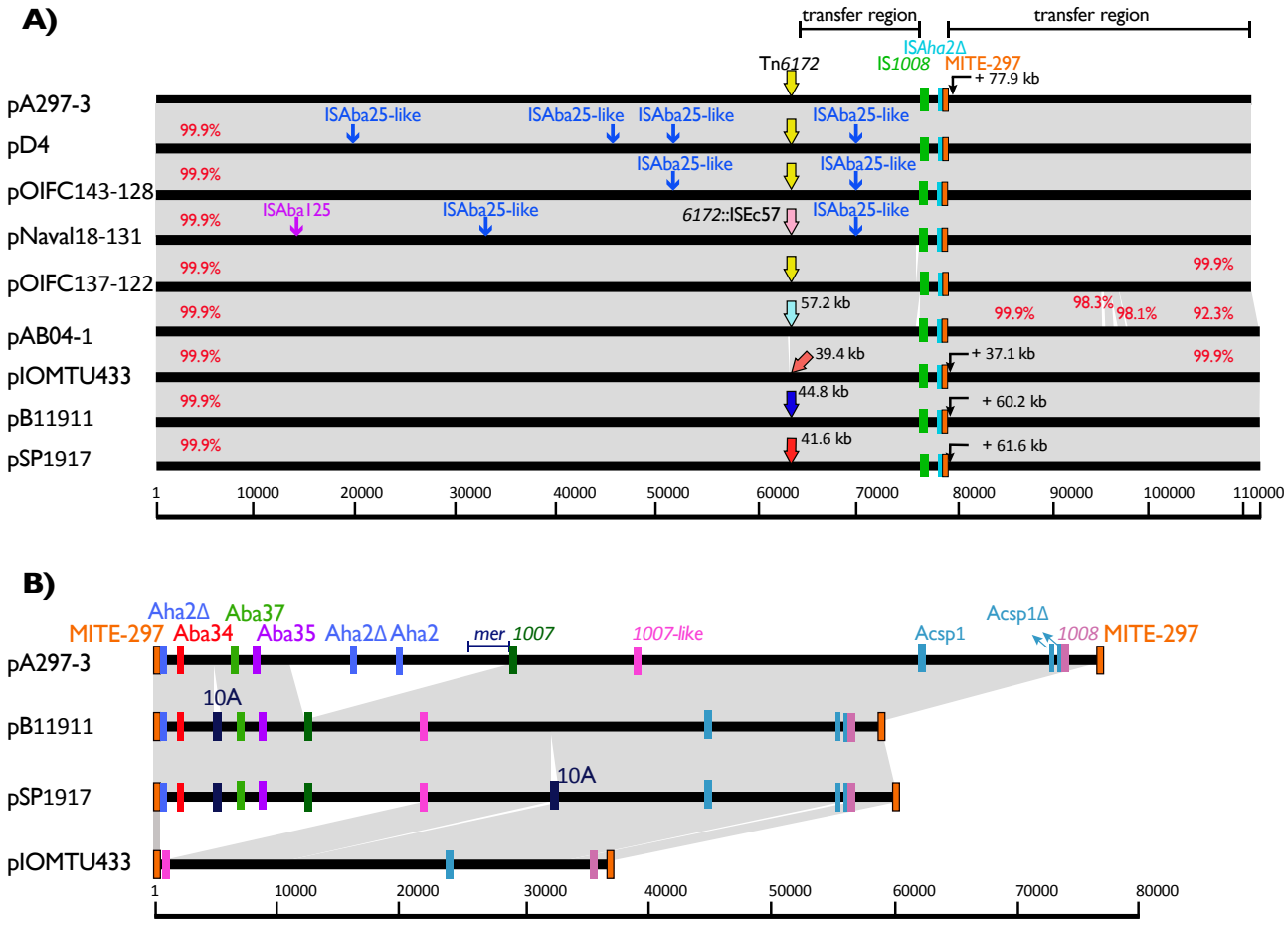

Fig. 4. Backbone comparison of plasmids related to pA297-3. A) represents the comparison of the main part of the backbone and B) indicates the segment between MITE-297 copies. Thick black horizontal bars represent plasmid backbones and sections filled gray show regions with various identities. Thick vertical arrows represent Tn*6172* and its other variants. Thin vertical arrows on pD4, pOIFC143-128 and pNaval18-131 represent ISAba125 and ISAba25-like insertions in the backbone. Boxes filled green, turquoise and orange represent IS*1008,* ISAha2Δ and MITE-297, respectively, which are present in all plasmids shown. Thin arrows pointing the sequence adjacent to the MITE-297 indicate the presence of additional segments of different lengths. Scale bar is also shown below with numbers indicating bp. Other boxes filled with various colors, of the section B, indicate insertion sequences, indicated above.